scientific reports

Check for updates

OPEN

Berberine inhibits the *tarO* gene to impact MRSA cell wall synthesis

Xuemei Gu[1,2], Fangfang Zhou[1,2], Mingming Jiang[1], Ming Lin[1], Yue Dai[1], Wei Wang[1], Zhongbo Xiong[1], Han Liu[1], Minyi Xu[1]✉ & Lei Wang[1]✉

Hospital and community-acquired infections caused by Methicillin-resistant *Staphylococcus aureus* (MRSA) have emerged as a significant public health challenge, highlighting the urgent need for novel antibiotics. In response, the antibacterial properties of natural products derived from traditional plants are being investigated as potential treatments for multidrug resistance. This study demonstrates the potent antibacterialimoact of Berberine (BBR), a compound derived from traditional Chinese medicine, against the community-associated MRSA (CA-MRSA) strain USA300 LAC. Through a comprehensive series of in vitro antibacterial experiments and gene-level investigations, we discovered that BBR compromises the integrity of the USA300 LAC cell wall structure. This mechanism of action is likely attributed to the inhibition of the *tarO* gene, which encodes a critical enzyme in the initial stage of wall teichoic acid (WTA) biosynthesis, thereby suppressing WTA synthesis, an essential component of the cell wall. Additionally, BBR upregulates the expression of lytic enzymes LytM and SsaA, resulting in accelerated hydrolysis of peptidoglycan, a major structural element of the cell wall. This disruption ultimately leads to the destruction of the USA300 LAC cell wall. Moreover, combined antibacterial assays reveal that BBR synergistically enhances the antibacterial effect of Oxacillin against USA300 LAC. Overall, our findings elucidate the antibacterial mechanism of BBR, a traditional Chinese medicine monomer, against MRSA and highlight its promising potential for clinical application in the treatment of MRSA.

Keywords Berberine, Methicillin-resistant *Staphylococcus aureus*, *tarO*, Cell wall, Inhibitory mechanism

Methicillin-resistant *Staphylococcus aureus* (MRSA) is a highly pathogenic and widely prevalent bacterium resistant to all clinically used β-lactam antibiotics. Vancomycin is the primary antimicrobial agent used for clinical treatment of MRSA infections. MRSA resistance is attributed to the production of a unique penicillin-binding protein (PBP), PBP2a, encoded by the *mecA* resistance gene. PBP2a has a reduced affinity for β-lactam antibiotics, allowing the bacteria to maintain peptidoglycan synthesis even in the presence of these drugs, thereby conferring resistance[1]. The development of novel antibacterial drugs remains a critical and challenging area of research.

Medicinal plants, particularly those used in traditional Chinese medicine, are valuable sources of potential antibacterial compounds and play a crucial role in discovering new antibiotics. Previous studies have demonstrated the favorable antibacterial effects of extracts derived from Chinese medicinal herbs, such as *Coptis chinensis* (Huang Lian) and *Phellodendron amurense* (Huang Bai), against MRSA[2]. Berberine (BBR), the primary component of these herbs, is an isoquinoline alkaloid known for its antibacterial properties against common pathogens, including *Candida albicans* and *S. aureus*[3]. The earlier investigations also revealed promising antibacterial effects of BBR against MRSA[4]. BBR has been shown to increase ion leakage in MRSA cells, alter the fatty acid composition, and disrupt cell membrane integrity[5]. Moreover, when combined with plant extract—paclitaxel, BBR effectively inhibited the transcription of biofilm-related genes (*sarA*, *cidA*, *icaA*) and reduced biofilm formation[6]. Transcriptome sequencing has identified BBR's antibacterial effects against MRSA, including the regulation of cell wall hydrolysis genes, increased cell membrane permeability, and reduced expression of virulence factors like leukocidin[7]. Additionally, transmission electron microscopy showed that BBR caused severe damage to the MRSA cell structure, leading to bacterial lysis and death[8]. However, research into the detailed mechanisms by which BBR affects the bacterial cell wall remains limited.

The bacterial cell wall is a complex structure crucial for maintaining cellular morphology. In *S. aureus*, the cell wall primarily consists of teichoic acid and peptidoglycan. Teichoic acid is divided into wall teichoic acid (WTA) and lipoteichoic acid (LTA)[9]. The WTA biosynthetic pathway can be classified into two groups: early WTA genes (*tarO*, *tarA*, and *mnaA*) and late WTA genes involved in WTA synthesis and extracellular

[1]Department of Clinical Laboratory, Shanghai Eighth People's Hospital, Shanghai, China. [2]Xuemei Gu and Fangfang Zhou contributed equally to this work. ✉email: mx8712@126.com; wolei6610@126.com

transport[10,11]. The *tarO* gene, a pivotal component in the initial stage of WTA biosynthesis, promotes the production and processing of lipid-linked sugars that subsequently bind to peptidoglycan, strengthening the cell wall[12]. Although staphylococci lacking WTA can survive, their growth is impeded[13].

Peptidoglycan, a crucial component of the cell wall, provides mechanical strength and protects bacterial cells. Bacteria use hydrolytic enzymes, known as autolysins, to perform essential physiological functions, including cell wall remodeling, cell division, biofilm formation, and surface adhesion[14]. The activity of these enzymes is meticulously regulated. *Staphylococcus aureus* harbors numerous peptidoglycan hydrolases, including SsaA, AtlA, LytM, and LytH[15]. LytM, a glycine N-acyltransferase of the Zn^{2+}-dependent M23 family, specifically cleaves peptide bonds between glycine and alanine in the cell wall peptidoglycan of *S. aureus*, resulting in bacterial lysis[16]. SsaA, a member of the Cysteine-Histidine-dependent Amidohydrolases/Peptidases (CHAP amidase) family, features enzymes like LysK and LytA, which possess D-alanyl-glycyl endopeptidase activity. Consequently, bacterial autolysins hold potential as therapeutic agents against *S. aureus* infections[17]. Prior research has indicated that cranberry extract alters the *S. aureus* transcriptome by upregulating genes such as *lytM*, *vraR/S*, and *murZ*, while inhibiting bacterial peptidoglycan biosynthesis[18]. However, the impact of BBR on peptidoglycan and its associated hydrolases in *S. aureus* has not been explored.

Building on previous studies, the current investigation aims to further elucidate the mechanism by which BBR disrupts the bacterial cell wall. Previous studies have identified *tarO* as a key gene in the initial stage of WTA synthesis in MRSA cell walls, and inhibition of *tarO* can reduce the expression of bacterial virulence genes and restore bacterial susceptibility to β-lactam antibiotics[10,19]. Additionally, protein-small molecule docking simulations revealed a strong binding affinity between berberine and the TarO protein. Based on these findings, the study focuses on a comprehensive investigation of TarO. Techniques such as qRT-PCR, WTA-PAGE electrophoresis, and homologous recombination were employed to assess the effects of berberine on MRSA cell wall biosynthesis. This comprehensive examination seeks to deepen the understanding of the antibacterial mechanism of BBR against MRSA.

Results

Significant antibacterial activity of BBR against USA300 LAC in vitro

The minimum inhibitory concentration (MIC) of BBR against USA300 LAC was 128 μg/mL, while the minimum bactericidal concentration (MBC) was 512 μg/mL. The effect of varying BBR concentrations on the growth rate of USA300 LAC was evaluated by measuring absorbance values at 600 nm. As shown in Fig. 1D, bacterial proliferation was nearly halted at 256 μg/mL BBR, while 128 μg/mL and 64 μg/mL BBR significantly inhibited growth. For LIVE/DEAD staining, bacteria treated with different BBR concentrations were analyzed. Active bacteria were stained green, while dead bacteria were stained red (Fig. 1A). Flow cytometry analysis revealed a dose-dependent increase in the percentage of dead bacteria. At 64 μg/mL BBR, the percentage of dead bacteria was relatively low (2.77%), whereas at 128 μg/mL and 256 μg/mL, the percentages of dead bacteria were 15.54% and 72.38%, respectively (Fig. 1B). These results demonstrate that BBR not only effectively inhibits MRSA growth but also demonstrates bactericidal activity, especially at higher concentrations (Fig. 1C).

Significant disruptive effect of BBR on USA300 LAC cell structure

To assess possible deformations in the bacterial cell surface, including collapse, protrusions, or breakage, scanning electron microscopy (SEM) was utilized to examine the morphological structure of USA300 LAC. The impact of three different BBR concentrations (low: 32 μg/mL, medium: 128 μg/mL, and high: 512 μg/mL) on bacterial cell morphology was examined. The findings revealed that under low concentrations of BBR, the bacterial structure remained relatively intact. The cell surface became increasingly irregular at a medium concentration (128 μg/mL), eventually leading to cell disintegration. At high concentrations (512 μg/mL), the bacterial cells exhibited severe structural damage and lysis (Fig. 2).

BBR affects cell wall WTA synthesis by inhibiting *tarO* gene expression in USA300 LAC

WTA biosynthesis requires the participation of *tarO*, *tarA*, *tarG*, *tarH* and *mnaA* genes. *tarO* has been identified as a pivotal gene in the initial step of WTA synthesis within the MRSA cell wall. To explore the effect of BBR on *tarO* expression, we performed qRT-PCR analysis, which demonstrated that BBR significantly inhibited *tarO* gene expression in USA300 LAC (Fig. 3A). We hypothesized that BBR might affect WTA synthesis in the cell wall by inhibiting the expression of the *tarO* gene in USA300 LAC. To validate this hypothesis, we generated a USA300 LAC mutant (Δ*tarO*), in which the *tarO* gene was knocked out, and a complemented strain R-*tarO*. qRT-PCR analysis further confirmed that 64 μg/mL BBR significantly reduced the expression of the *tarO* gene in the complemented strain R-*tarO* (Fig. 3B). We utilized WTA-PAGE electrophoresis to examine the impact of BBR treatment on the content of USA300 LAC-WT WTA. The results illustrated (Fig. 3C) a concentration-dependent decline in WTA content as BBR concentration increased, with the most significant reduction observed at concentrations of 128 μg/mL and 64 μg/mL BBR Further analysis showed that BBR decreased WTA expression in both USA300 LAC-WT and R-*tarO* complemented strains. In the Δ*tarO* mutant, WTA production was completely abolished (Fig. 3D). Molecular docking between BBR and the target protein was conducted utilizing AutoDock Vina to explore their interaction. The more negative the binding energy, the more stable the ligand-receptor binding. Binding energies of less than −4.25 kcal/mol, −5.0 kcal/mol, and −7.0 kcal/mol correspond to weak, good, and strong binding activity, respectively, between the ligand and receptor[20]. Streptavidin-Biotin has a −20 kcal/mol binding energy and is considered a very strong interaction. The results showed that BBR, a small molecule, exhibited strong binding affinity with the TarO protein, with an optimal binding energy of −8.5 kcal/mol. To further investigate the interaction, PyMOL v2.5.4 was used to analyze the hydrogen bonding between berberine and TarO. The 3D interaction maps revealed that BBR forms hydrogen bonds with TarO's LYS-38 and LEU-206, ensuring stable binding (Fig. 3E). Meanwhile, BBR decreased

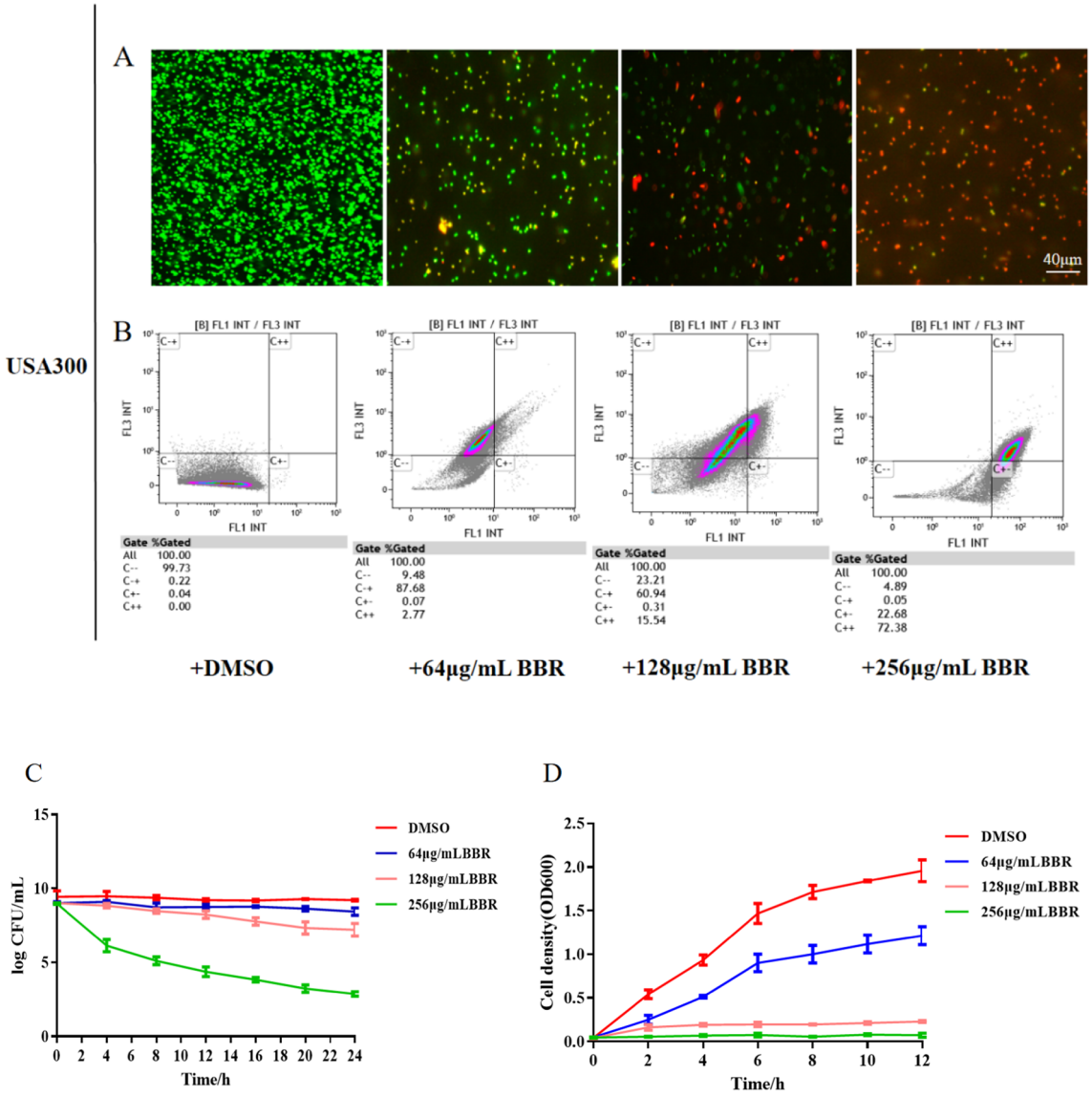

Fig. 1. In vitro antibacterial activity of BBR. (**A**) Detection of bacterial viability after treatment with different concentrations of BBR (Green: active bacteria, Red: dead bacteria). (**B**) Flow cytometry analysis of live/dead bacteria after BBR treatment(C−− for live bacteria, C++ for dead bacteria). (**C**) The time-killing curve of USA300 LAC with different concentrations of BBR (**D**) Growth curve of USA300 LAC under the influence of different concentrations of BBR.

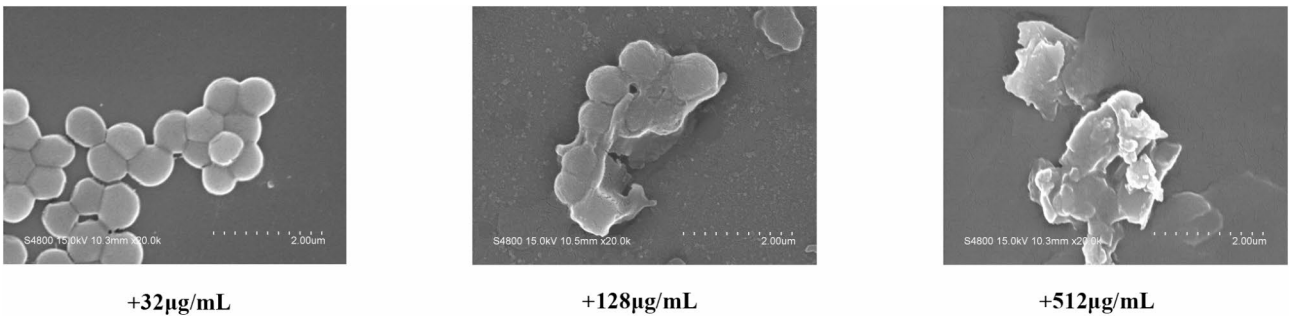

Fig. 2. Observation by SEM of USA300 LAC bacterial strain.

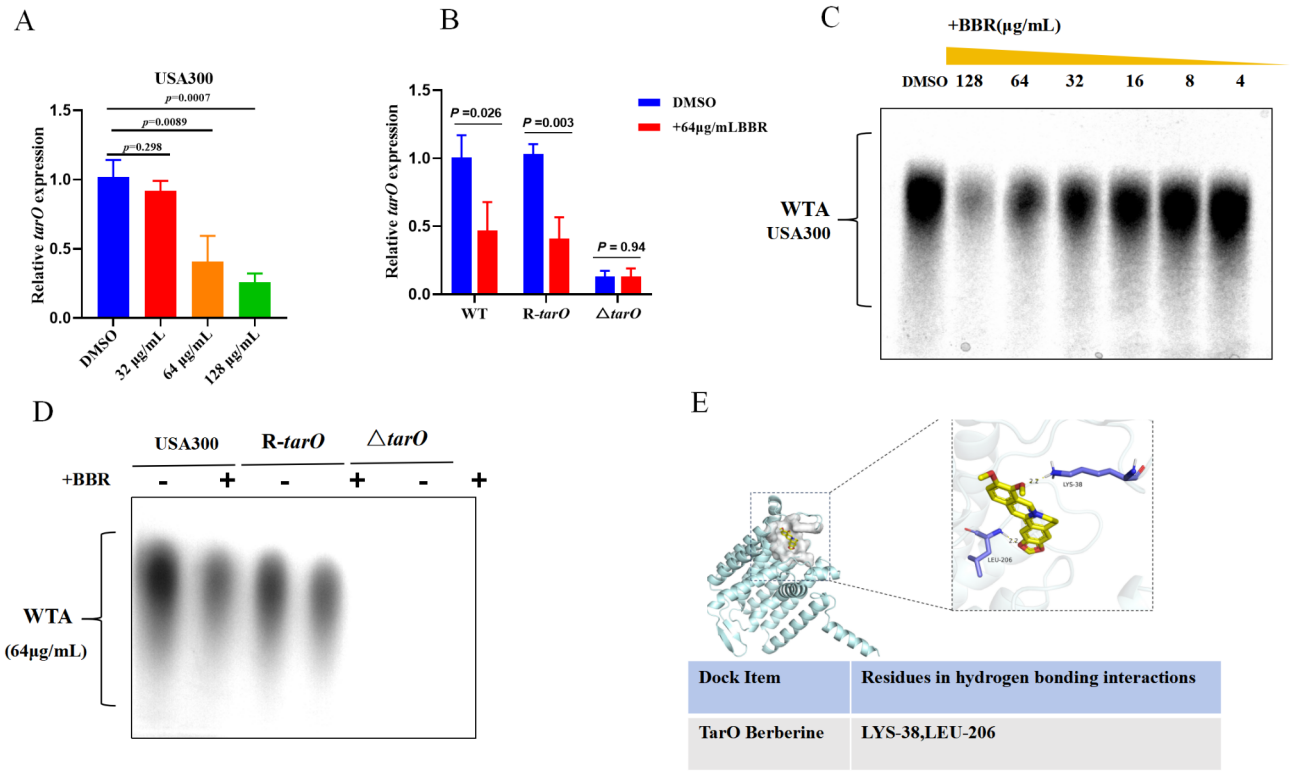

Fig. 3. Changes in WTA content and *tarO* gene expression in the strain after BBR treatment were assessed. (**A**) qRT-PCR was utilized to detect alterations in *tarO* gene levels in USA300 LAC following 3 h of treatment with varying concentrations of BBR. (**B**) qRT-PCR analysis was carried out to assess *tarO* gene levels in USA300 LAC-WT, complemented strain R-*tarO*, and Δ*tarO* mutant after 3 h of BBR treatment. (**C**) WTA-PAGE analysis was performed on USA300 treated with different concentrations of BBR. (**D**) WTA-PAGE analysis was conducted after treatment with 64 μg/mL BBR in USA300 LAC-WT, R-*tarO*, and Δ*tarO* strains. (**E**) 3D molecular docking diagram of berberine and TarO. (Data represents the average of three independent experiments ± SD; statistical analysis performed utilizing a one-way ANOVA).

the biosynthesis of WTA by inhibiting the expression of *tarO*, which indirectly reflected the effect of BBR on the enzyme activity of TarO. These findings provide evidence that BBR inhibits WTA biosynthesis by suppressing the expression of the *tarO* gene or affecting the activity of the TarO protein.

Increased sensitivity of Δ*tarO* mutant to OXA and BBR

Further sensitivity tests were performed utilizing antibiotics targeting the cell wall. In Fig. 4, bacterial suspensions of USA300 LAC-WT, R-*tarO* complemented strain, and Δ*tarO* mutant were exposed to OXA or BBR, then spotted on agar plates and incubated for 24 h at 37 °C to observe bacterial growth. The results showed that the growth of the Δ*tarO* mutant without any treatment (DMSO only) was lower than that of other strains (USA300 LAC and R-*tarO*). Furthermore, Δ*tarO* mutants showed increased sensitivity to β-lactam antibiotic, Oxacillin, while wild strains and complementary strains were able to grow at the test concentration (1 μg/mL). Moreover, BBR demonstrated a more pronounced inhibitory effect on the Δ*tarO* mutants compared to the WT strain (Fig. 4A), with corresponding MIC values significantly decreased (Table 1).

The Inhibition of *tarO* by BBR May potentially enhance the synthesis of cell wall peptidoglycan hydrolases *lytM* and *ssaA*

Previous transcriptomic analysis revealed a significant upregulation of these hydrolases, namely *ssaA* and *lytM*, in response to BBR treatment[7]. qRT-PCR validation of *ssaA* and *lytM* gene expression in the three strains following BBR treatment demonstrated that BBR stimulated the expression of *ssaA* and *lytM* genes in the wild-type and complemented strains. Conversely, no significant differences were found in the expression levels of these genes in the Δ*tarO* mutant (Fig. 5A–C). Based on these findings, it is hypothesized that BBR enhances the synthesis of *ssaA* and *lytM* by affecting the activity of TarO. Relevant literature suggests that *lytM* is regulated by the Agr system effector RNAIII[18]. Our subsequent studies also indicated that BBR can inhibit the expression of RNAIII, and we plan to continue investigating the underlying mechanisms involved.

Synergistic antibacterial effect of BBR in combination with OXA on USA300 LAC

A spot dilution assay was conducted to evaluate the bactericidal activity of USA300 LAC treated with DMSO, BBR alone, OXA alone, and the combination of BBR and OXA. Serial dilutions of the treatments were plated on

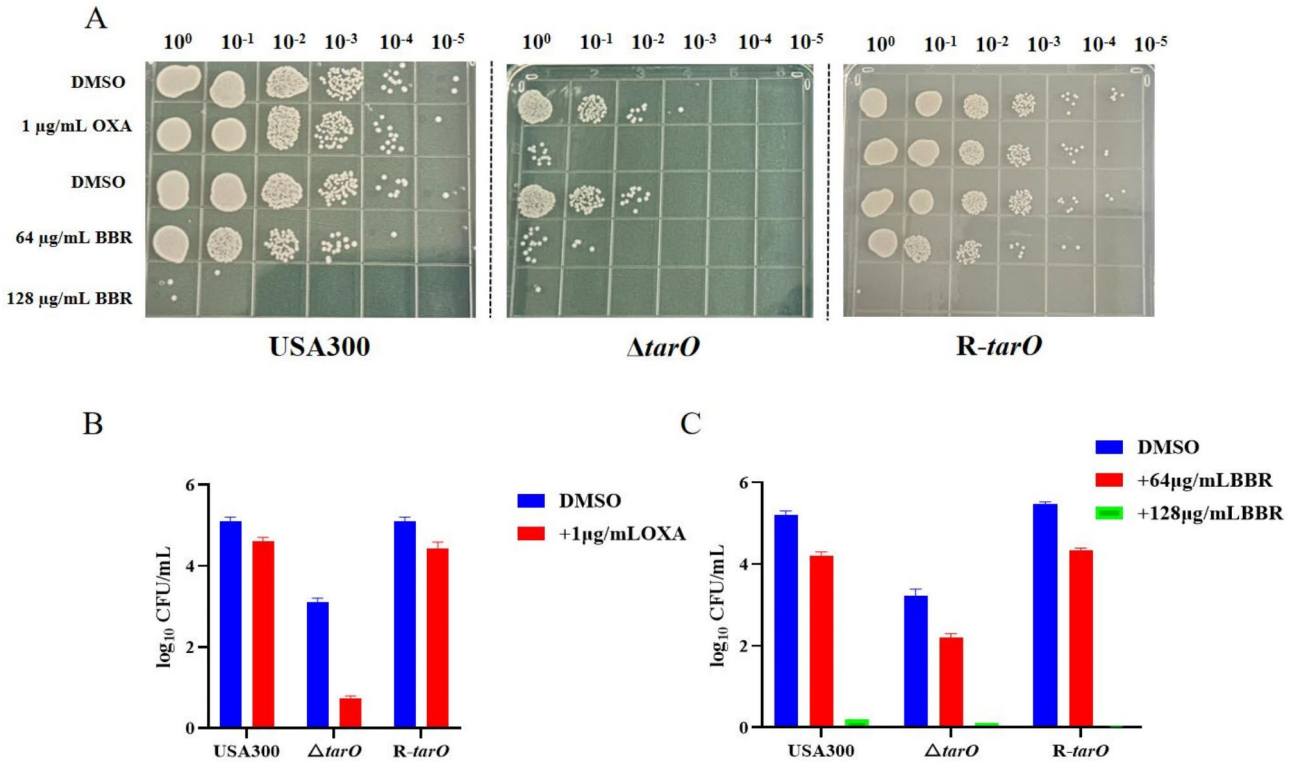

Fig. 4. Antibacterial effects of BBR and OXA on three strains. (**A**) Growth of USA300 LAC-WT, R-*tarO* complemented strain, and Δ*tarO* mutant under different conditions (DMSO, 1 μg/mL OXA, 64 μg/mL BBR, 128 μg/mL BBR) on TSA agar plates. (**B**) Colony count of USA300 LAC-WT, R-*tarO* complement strain, Δ*tarO* mutant after OXA treatment. (**C**) Colony count of USA300 LAC-WT, R-*tarO* complement strain, Δ*tarO* mutant after BBR treatment.

	BBR	OXA
WT	128	16
R-*tarO*	128	8
Δ*tarO*	64	0.5

Table 1. MIC of Berberine and Oxacillin against three strains (μg/mL).

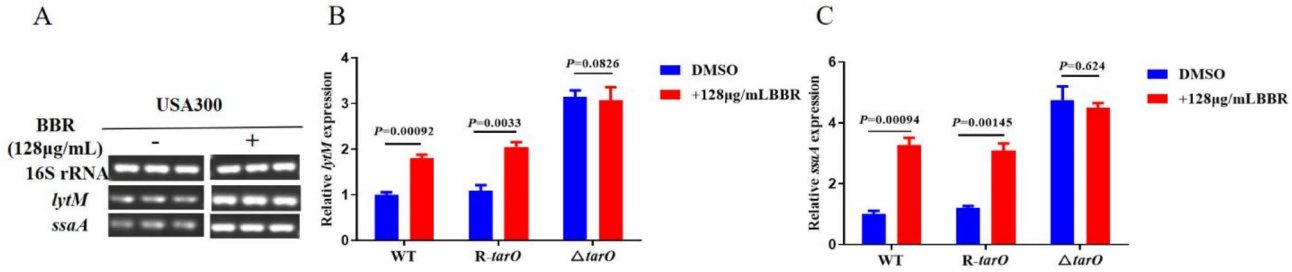

Fig. 5. Regulation of *lytM* and *ssaA* by BBR in USA300 LAC. (**A**–**C**) qRT-PCR analysis of changes in *lytM* and *ssaA* gene levels after 3 h of BBR treatment in the wild-type, complemented strain R-*tarO*, and Δ*tarO* mutant (Data represent the average of three independent experiments ± SD, statistical analysis performed utilizing a two-sample t-test).

agar plates and incubated at 37 °C for 18 h. The results demonstrated a significant synergistic antibacterial effect when BBR was combined with OXA, with the most pronounced effect observed at 64 μg/mL BBR combined with 4 μg/mL OXA (Fig. 6A). To further evaluate the bacteriostatic effect, a Fractional Inhibitory Concentration (FIC) analysis utilizing the checkerboard method was conducted. The FIC value was 0.75, indicating an additive combined antibacterial effect of BBR and OXA. Additionally, qRT-PCR analysis indicated that BBR significantly downregulated the expression levels of the peptidoglycan synthesis gene *pbp2* and the resistance gene *mecA* in USA300 LAC after a 3-hour treatment (Fig. 6B).

BBR demonstrates low toxicity

To assess the toxicity of BBR, L929 mouse fibroblasts were exposed to varying concentrations of BBR for 24 h. Cell morphology and quantity were observed under a microscope. The results showed no significant differences in either cell morphology or quantity when comparing the treated groups to the control group (Fig. 7A). Furthermore, cytotoxicity was measured utilizing MTT assays after exposing L929 cells to BBR for 24 h. No cytotoxic effects were observed, even at very high concentrations (256 μg/mL), with 85.04% of cells remaining viable after 24 h (Fig. 7B). These findings confirm the safety of BBR.

Discussion

The clinical application of traditional Chinese medicine in combating infectious diseases has gained significant attention, especially in the context of investigating the antibacterial properties of Chinese herbal medicines and their components against drug-resistant bacteria commonly encountered in clinical settings. This study conducted a series of in vitro experiments that clearly demonstrated the potent antibacterial efficacy of BBR against MRSA. The results illustrated that a concentration of 128 μg/mL of BBR effectively inhibited USA300 LAC growth, with bacterial mortality increasing progressively as the BBR concentration was raised (Fig. 1). SEM further revealed that higher concentrations of BBR led to significant damage to the cell structure of USA300 LAC (Fig. 2).

Similar to the cell wall components of gram-positive bacteria, the MRSA cell wall is primarily composed of peptidoglycan (PG) and teichoic acid [lipoteichoic acid (LTA) and wall teichoic acids (WTA)]. PG significantly influences cell division and proliferation, while WTA is closely associated with the pathogenicity and drug resistance of *S. aureus*[21]. TarO is the key enzyme in the early stage of WTA biosynthesis. Inhibiting TarO expression impedes WTA synthesis, resulting in bacterial cell wall lysis and exerting an antibacterial effect[11]. Through investigating the WTA biosynthesis pathway and conducting molecular docking studies, we found that BBR binds strongly to TarO, which may alter its enzyme activity. qPCR results further confirmed that BBR inhibits the expression of the *tarO* gene, leading to a decrease in WTA biosynthesis. This finding was cvalidated utilizing a Δ*tarO* mutant and the complemented strain (R-*tarO*), constructed via homologous recombination (Fig. 3). Previous studies have shown that Δ*tarO* mutants exhibit reduced growth rates, irregular cell shapes, and impaired bacterial division due to the disruption of WTA synthesis, ultimately resulting in compromised resistance to environmental stress[4,22]. The findings suggest that BBR may promote the synthesis of peptidoglycan hydrolases, such as *lytM* and *ssaA*, in USA300 LAC by inhibiting the activity of the TarO (Fig. 5),

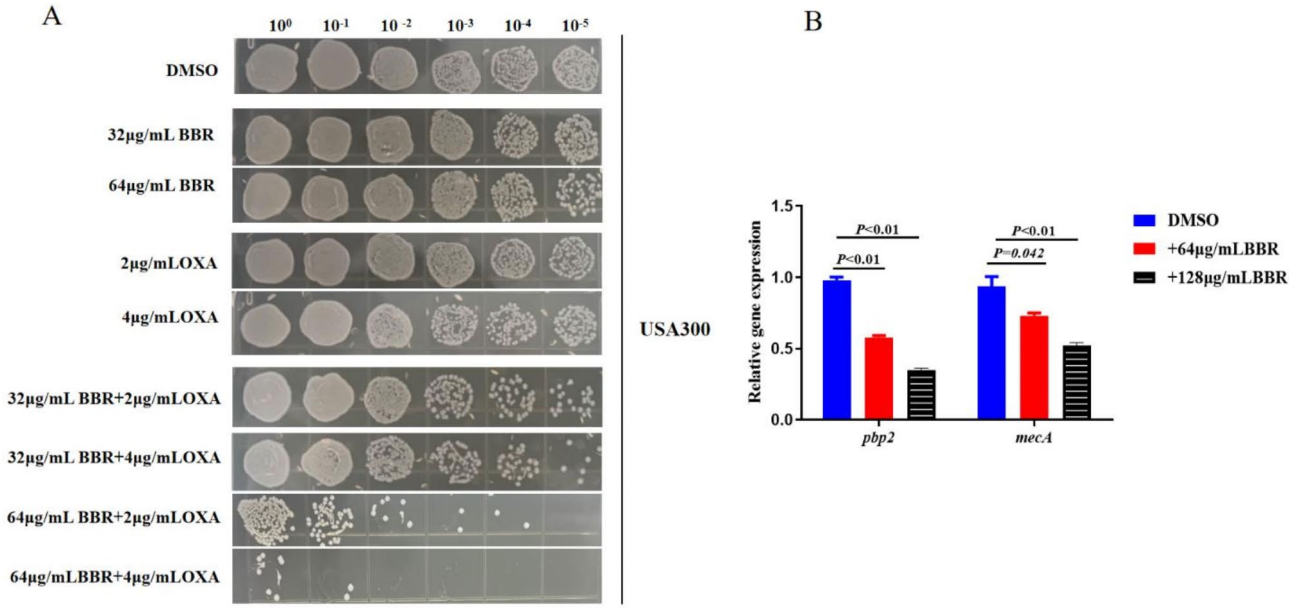

Fig. 6. Synergistic antibacterial effect of BBR in combination with OXA on USA300 LAC. (**A**) Spot dilution assay to observe the combined antibacterial effect of BBR and OXA. (**B**) qRT-PCR analysis of changes in *pbp2* and *mecA* gene mRNA levels after 3 h of BBR treatment in USA300 LAC (Statistical analysis performed utilizing a two-sample t-test.).

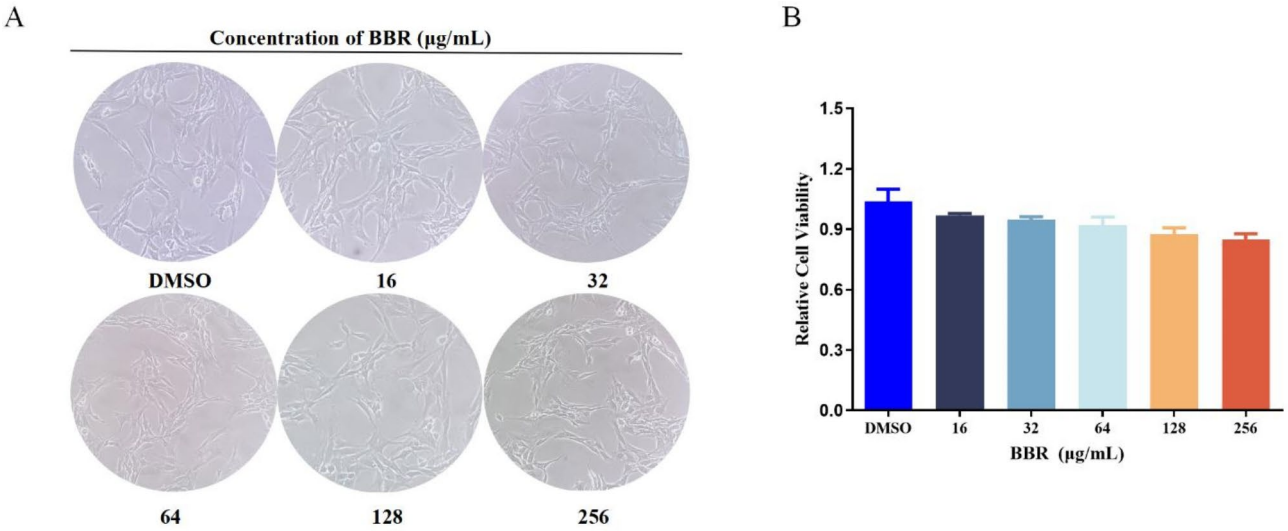

Fig. 7. Safety evaluation of BBR. (**A**) Toxicity of different concentrations of BBR on L929 mouse fibroblasts. (**B**) The activity of different amounts of L929 with or without BBR treatment (16 μL DMSO was added into 2 mL medium for 125-fold dilution as the control group in this experiment).

Gene	Primer sequence (5′–3′)	Source
ssaA-RT-F	ATCAAACAACACGCAATCAC	[32]
ssaA-RT-R	TGCCACCTACTCTGTCAAAT	
lytM-RT-F	TACAAGCAGGTTGGAGTA	[18]
lytM-RT-R	GTGTACGTGAGGCGCTGT	
tarO-RT-F	TTCCATCCTGCCAAAATA	Self-designed
tarO-RT-R	GAATGGAACTGCTAAGATAACA	
pbp2-RT-F	GATTTAAACTTAGCGGAAGAAGC	[10]
pbp2-RT-R	TGTTTTTACGATCTTCAGCAGC	
mecA-RT-F	GATTATGGCTCAGGTACTGCTATCC	[32]
mecA-RT-R	ATGAAGGTGTGCTTACAAGTGCTAA	
16S rRNA-RT-F	CTGTGCACATCTTGACGGTA	[18]
16S rRNA-RT-R	TCAGCGTCAGTTACAGACCA	

Table 2. Primer pairs used in RT-PCRs.

thereby facilitating peptidoglycan hydrolysis. Lu[10] observed similar results, showing upregulation of ssaA and lytM expression upon deletion of the *tarO* gene. SsaA and LytM possess potential WalKR binding sites, and the WalKR system directly governs bacterial cell wall hydrolysis[23]. High concentrations of BBR likely increase the interaction between SsaA, LytM, and WalR, enhancing the WalKR system's ability to degrade the bacterial cell wall, ultimately leading to cell wall rupture and bacterial death.

Additionally, Orihuela et al.[24] discovered that increased production of four peptidoglycan hydrolases, including SceD, SsaA, LytM, and AtlA, accelerated the degradation of the cell wall of *S. aureus*, thereby reducing oxacillin resistance. The synthesis of PG and WTA is closely interconnected, and disruption of WTA synthesis can impair PG synthesis, ultimately reducing resistance to β-lactam antibiotics[25]. In our study, we observed a notable synergistic antibacterial effect when BBR was combined with OXA, while a significantly down-regulated impact on the expression levels of *pbp2* and *mecA* genes was observed (Fig. 6A,B). Previous studies have suggested that WTA deficiency may result in the mislocalization of PBP2a or PBP4 in USA300 LAC, leading to the displacement of PBP2 protein across the cell membrane and resulting in reduced peptidoglycan cross-linking[10,26]. It is plausible that BBR not only enhances bacterial peptidoglycan hydrolysis but also inhibits WTA biosynthesis, thereby affecting the localization of PBPs and compromising cell wall integrity. The combination of BBR with OXA, which has a high affinity for PBP2 and inhibits bacterial peptidoglycan synthesis, is likely to produce a synergistic antibacterial effect. Nonetheless, further experiments are warranted to validate this hypothesis.

Previous studies have shown that BBR damages the MRSA cell structure through transcriptome sequencing and electron microscopy, but the underlying mechanism remained unclear[7]. To further investigate the mechanism of berberine on the bacterial cell wall, we demonstrate that BBR effectively inhibits the biosynthesis of WTA, a crucial component of the cell wall, by suppressing the expression of the *tarO* gene and interacting with the TarO

enzyme in this study. Additionally, BBR promotes the upregulation of peptidoglycan hydrolase genes, including *lytM* and *ssaA*, which accelerates the hydrolysis of peptidoglycan, the primary structural component of the cell wall. Consequently, the cell wall structure of USA300 LAC is disrupted. This study provides further insight into the molecular mechanism by which BBR impairs the MRSA cell wall. Furthermore, the combination of BBR with OXA enhances bacterial sensitivity to OXA, resulting in a synergistic antibacterial effect. In conclusion, our findings suggest that BBR is a potent inhibitor and, when combined with existing β-lactam antibiotics, has the potential to restore the therapeutic efficacy of this important antibiotic class against MRSA.

Materials and methods

Bacterial strains, cells, and growth conditions

The bacterial strain used in this study was USA300 LAC, provided by the LAN Lefu Research Group at the School of Pharmaceutical Science and Technology, Hangzhou Institute for Advanced Study, University of Chinese Academy of Sciences. To maintain plasmid resistance, USA300 LAC derivative strains were cultured in the presence of 80 μg/mL erythromycin (Sangon Biotech). *S. aureus* strains were grown at 37 °C with shaking at 250 rpm in tryptic soy broth (TSB, Difco) or on tryptic soy agar (TSA, Difco). L929 mouse fibroblast cells, used for cytotoxicity assessments, were cultured in RPMI-1640 medium containing 10% fetal bovine serum (FBS, Sigma-Aldrich, St. Louis, MO, USA) at 37 °C with 5% CO_2.

BBR and antibiotics

BBR was purchased from Beijing WoKe Biological Technology Co., Ltd. (Production batch number: XW20868312) and dissolved in dimethyl sulfoxide (DMSO). OXA was obtained from Shanghai Maclin Biochemical Technology Co., Ltd. (Production batch number: C15128755) and prepared in sterile deionized water.

MIC and MBC determination

BBR solution was serially diluted in Mueller-Hinton broth to final concentrations of 8, 16, 32, 64, 128, 256, 512, and 1024 μg/mL. Oxacillin was diluted in Mueller-Hinton broth to final concentrations of 0.125, 0.25, 0.5, 1, 2, 4, 8, 16, and 32 μg/mL. An inoculum was prepared by selecting 4–5 isolated colonies until achieving a turbidity equivalent to the 0.5 McFarland standard (1×10^8 CFU/mL). The bacterial suspension was then diluted to a concentration of 5×10^5 CFU/mL. Subsequently, 0.1 mL bacterial suspension and 0.1 mL berberine or antibiotic solution were added to each well, and the final volume was 0.2 mL. The plate was incubated overnight at 37 °C, and the lowest drug concentration that completely inhibited bacterial growth was determined as the MIC (Negative controls (no bacterial suspension) and positive controls (no BBR and OXA) were included in the experiment, which was repeated three times). The MIC of the *S. aureus* strains was determined utilizing broth microdilution by the Clinical and Laboratory Standards Institute(CLSI)[27].

Synergistic antibacterial assay

In a 96-well plate, 50 μL of different concentrations of berberine and oxacillin sodium solutions were arranged in rows and columns. An inoculum was prepared by selecting 4–5 isolated colonies until achieving a turbidity equivalent to the 0.5 McFarland standard (1×10^8 CFU/mL). The bacterial suspension was then diluted to a concentration of 5×10^5 CFU/mL. Subsequently, 0.1 mL bacterial suspension and 0.1 mL berberine or antibiotic solution were added to each well, and the final volume was 0.2 mL. After overnight incubation at 37 °C, the culture was diluted tenfold, and 10 μL of the diluted bacterial suspension was added to each well. The plate was air-dried and incubated at 37 °C for 24 h. The antibacterial effect of berberine in combination with oxacillin was assessed utilizing the FIC index, as described by Kumarihamy et al.[28]. Synergy was defined as an FICI of ≤ 0.5; antagonism was defined as an FICI > 2.0; an FICI of > 0.5 but ≤ 1.0 was regarded as additivity; and an FICI of > 1.0 but ≤ 2.0 was regarded as indifference. The experiment was repeated three times.

FIC = [A*]/[A] + [B*]/[B], where [A*] denotes the MIC of compound A in the presence of compound B, [A] represents the MIC of compound A alone, [B*] indicates the MIC of compound B in the presence of compound A, and [B] indicates the MIC of compound B alone.

Bacterial viability assay

The AAT Bioquest MycoLight™ Bacterial Viability Assay Kit was used for a two-color fluorescence assay to determine bacterial viability in both gram-positive and gram-negative bacteria. In this assay, a combination of MycoLight™ Green and propidium iodide stains was used. Living bacteria with intact cell membranes fluoresce green, while dead or dying bacteria with compromised cell membranes fluoresce red. The bacterial medium was diluted to a concentration of 10^5 to 10^8 cells/mL utilizing 0.85% NaCl or an appropriate buffer. A sufficient volume of suspension was prepared to provide at least 500 μL per test for flow cytometry (Beckman Coulter, USA). The two dyes were mixed in a 1:1 ratio, and 4 μL of the dye working solution (AAT Bioquest, USA) was added to each ml of the bacterial suspension. The mixture was incubated at room temperature for 15 min and protected from light. The stained bacterial cells were subsequently analyzed by flow cytometry.

Time-killing assay

The bacterial suspension in the logarithmic growth phase (OD600 ≈ 0.5, about 1.5×10^9 CFU/mL) was prepared in TSB medium, and different concentrations of berberine were added for co-cultivation. Samples were taken at 4, 8, 16, 20, and 24 h of incubation. After sampling, the samples were serially diluted by a factor of 10, up to 10^{-8} times. A 100 μL aliquot of each dilution was plated on TSB agar plates and incubated for 24 h. Colony counts were recorded and expressed as CFU/mL[29,30].

SEM

For SEM analysis, the bacterial samples were fixed in 2.5% (v/v) glutaraldehyde (GLU) in 0.1 M phosphate-buffered saline (PBS) for 2 h. After fixation, the samples were rinsed twice with PBS for 10 min each time, followed by dehydration in a graded alcohol series. The dehydrated samples were then placed in 100% acetone as a transitional liquid before being transferred to the Critical Point Drier (CPD E3000/E3100, Quorum Technologies). The samples were subsequently coated with gold utilizing a JFC-1100E Ion Sputter (Jeol). For coating, the materials were mounted on conductive carbon adhesive tabs (Electron Microscopy Sciences). Morphological analysis was performed utilizing an SEM (JSM-5410).

Molecular docking

Molecular docking was utilized to investigate the potential binding mode of BBR with TarO. The chemical structure of BBR was obtained from PubChem (https://pubchem.ncbi.nlm.nih.gov/), and the binding affinity was analyzed utilizing AutoDock Vina 1.2.5. Core targets corresponding to the TarO protein were identified by searching the NCBI database (https://www.ncbi.nlm.nih.gov/protein/QLH97459.1). The amino acid sequence was used to predict the structure of the core target protein with AlphaFold, and the protein 3D model structure was downloaded in PDB format. PyMOL software was first used to remove solvents and organics from the protein structures. AutoDock software (v1.5.6) was then employed for molecular docking, and the results were visualized utilizing PyMOL software (v2.5.4).

WTA extraction and the polyacrylamide gel electrophoresis (PAGE) analysis

For WTA extraction, 20 mL of bacterial culture with an initial OD600 ≈ 0.1 (about 3×10^8 CFU/mL)was incubated overnight at 37 °C in the presence of berberine. The turbidity of the bacterial solution was homogenized by detecting OD value, and the WTAs were extracted[31]. The gel was run in a Bio-Rad Protean II xi electrophoresis apparatus at 4 °C with constant current (80 mA) in Tris-Tricine running buffer (0.1 M Tris base, 0.1 M Tricine, pH 8.2) for several hours. After electrophoresis, WTA was visualized by staining with Alcian blue silver staining methods.

RNA extraction and qRT-PCR

Bacterial cultures were diluted to an initial OD600 ≈ 0.1 (about 3×10^8 CFU/mL), treated with different concentrations of BBR, and incubated at 37 °C for 3 h. DMSO was used for the control group. RNA extraction was performed utilizing the Qiagen RNeasy kit according to the manufacturer's instructions. qRT-PCR was conducted utilizing a two-step method. First, RNA was reverse-transcribed into cDNA utilizing the M-MuLV First Strand cDNA Synthesis Kit (Sangon Biotech). Real-time quantitative PCR was then performed utilizing 2× SG Fast qPCR Master Mix (Low Rox) (Sangon Biotech) on a QuantStudio 5 Applied Biosystems (ABI) fluorescence quantitative PCR instrument (Thermo Fisher Scientific). Gene expression changes were calculated utilizing the $2^{-\Delta\Delta Ct}$ method. All experiments were performed with three independent biological replicates, and each tested gene was tested in triplicate for technical replicates.

Spot dilution assay

LB solid medium (500 mL) was prepared by dissolving 5 g NaCl, 2.5 g beef extract, 5 g tryptone, and 7.5 g agar and then autoclaved at 121 °C. The mixture was poured into Petri dishes and allowed to solidify. Bacterial suspensions were prepared by picking single colonies and incubating overnight at 37 °C with shaking at 250 rpm. The cultures were adjusted to an initial OD600 ≈ 0.1 (about 3×10^8 CFU/mL). Tubes containing berberine were placed in a 37 °C, 250 rpm shaking incubator overnight. After incubation, the cultures were serially diluted 10-fold, and 10 µL of the PBS-diluted bacterial suspension was spotted onto the Petri dish. The dish was air-dried and incubated at 37 °C for 24 h.

Construction of gene deletion mutants

To construct the *tarO* deletion mutant (Δ*tarO*), the upstream fragment (~ 1.1 kb) was amplified from *S. aureus* USA300 LAC genomic DNA utilizing the primers *tarO*-up-F and *tarO*-up-R (Table 3). The downstream fragment (~ 1.0 kb) was amplified utilizing the primers *tarO*-down-F and *tarO*-down-R (Table 3). The overlapping PCR was used to join the upstream and downstream fragments, and the resulting product was recombined with the plasmid pKOR1 utilizing primers *tarO*-up-F and *tarO*-down-R to obtain pKOR1::*tarO*. The plasmid was introduced into *Escherichia coli* DH5α, sequenced to verify the absence of unwanted mutations, and then electroporated into *S. aureus* RN4220 and subsequently into *S. aureus* USA300 LAC. PCR was performed to confirm the deletion of the target gene.

Primers	Primer sequence (5′–3′)	Purpose
tarO-up-F	GGGGACAAGTTTGTACAAAAAAGCAGGCTGTGAATGACAACTGAGAACTCTTC	For pKOR1::*tarO*
tarO-up-R	CCATACAGCTATGCTTTCATTCCTTATTCACCTTCATCGATATTAATTG	
tarO-down-F	GGAATGAAAGCATAGCTGTATGG	
tarO-down-R	GGGGACCACTTTGTACAAGAAAGCTGGGTGTCACACTTAATGGCGCTATTTG	
tarO-F	ACAATTAATATCGATGAAGGTGAATAA	For R-*tarO*
tarO-R	AGGGGGCCCACAGCTATGCTTTCATTCCCTATT	

Table 3. Primer pairs used in Plasmids[10].

Plasmids	Relevant genotype or characteristic	Source
pYJ335	*E. coli–S. aureus* shuttle vector, Cm^r, Erm^r	
pYJ335-1	A modified pYJ335 plasmid containing AscI and PspOMI restriction enzyme sites followed by the blunt-end EcoRV site of pYJ335	This study
R-*tarO*	pYJ335-1 derivative carrying *tarO* in the downstream of the xyl/tetO promoter	This study
pKOR1	Gene replacement vector for *S. aureus* genes, Amp^r, Cm^r	
pKOR1::*tarO*	pKOR1 derivative, for deletion of *tarO*	This study

Table 4. Plasmids used in this study.

Construction of gene complementation plasmids

To improve cloning efficiency, two restriction endonuclease sites (AscI and PspOMI) were introduced into the pYJ335 plasmid utilizing site-directed mutagenesis with the primers pYJ335-F and pYJ335-R. The resulting plasmid, pYJ335-1, contained restriction sites for EcoRV, AscI, and PspOMI. For the construction of the R-*tarO* plasmid, the *tarO* gene was amplified from *S. aureus* USA300 LAC genomic DNA utilizing the primers *tarO*-F and *tarO*-R (Table 3). The *tarO* PCR fragment was digested with PspOMI, and the pYJ335-1 plasmid was digested with EcoRV and PspOMI. The *tarO* gene was ligated downstream of the xyl/tetO promoter in pYJ335-1, resulting in the plasmid R-*tarO* (Table 4).

MTT assay

The cytotoxicity of BBR was measured by MTT assay in L929 cells. L929 cells (1×10^5 cells/mL) were cultured in 96-well plates for 24 h and then treated with different concentrations of BBR (0, 16, 32, 64, 128, and 256 μg/mL) for 24 h. After treatment, MTT solution was added to the cells and incubated for 4 h. The resulting MTT crystals were solubilized in dimethyl sulfoxide (Sigma-Aldrich). The optical density was measured at 490 nm utilizing a microplate reader (Epoch; BioTek, Winooski, VT, USA). The experiment was conducted three times.

Statistical analysis

Statistical analysis was performed utilizing GraphPad Prism 8.0 software. Data were analyzed by Student's t-test and one-way analysis of variance (ANOVA). A p value less than 0.05 was considered statistically significant (* $p < 0.05$, ** $p < 0.01$).

Data availability

All data generated or analysed during this study are included in this published article [and its supplementary information files].The datasets used and/or analysed during the current study available from the corresponding author on reasonablerequest.

Received: 26 September 2024; Accepted: 24 February 2025
Published online: 26 February 2025

References

1. Bilyk, B. L., Panchal, V. V., Tinajero-Trejo, M., Hobbs, J. K. & Foster, S. J. An Interplay of multiple positive and negative factors governs methicillin resistance in *Staphylococcus aureus*. *Microbiol. Mol. Biol. Rev.* **86**(2), e0015921 (2022).
2. Wang, X. et al. Berberine inhibits *Staphylococcus epidermidis* adhesion and biofilm formation on the surface of titanium alloy. *J. Orthop. Res.* **27**, 1487–1492 (2009).
3. Wei, G.-X., Xu, X. & Wu, C. D. In vitro synergism between berberine and miconazole against planktonic and biofilm *Candida cultures*. *Arch. Oral Biol.* **56**, 565–572 (2011).
4. Luo, J.-Y., Yan, D. & Yang, M.-H. Study of the anti-MRSA activity of *Rhizoma coptidis* by chemical fingerprinting and broth microdilution methods. *Chin. J. Nat. Med.* **12**, 393–400 (2014).
5. Zhang, X. et al. Berberine damages the cell surface of methicillin-resistant *Staphylococcus aureus*. *Front. Microbiol.* **11**, 621 (2020).
6. Guo, N. et al. The synergy of berberine chloride and totarol against *Staphylococcus aureus* grown in planktonic and biofilm cultures. *J. Med. Microbiol.* **64**, 891–900 (2015).
7. Zhou, F., Wang, L., Wang, W. & Lu, P. Effect of berberine on the whole genome transcription of methicillin-resistant *Staphylococcus aureus*. *Chin. J. Lab. Med.* **43**(05), 576–581 (2020).
8. Zhou, F., Gu, X., Wang, L. & Lin, M. The mechanism of berberine on methicillin resistant *Staphylococcus aureus* in vitro. *Chin. J. Prev. Med.* **57**(8), 1217–1221 (2023).
9. Xia, G., Kohler, T. & Peschel, A. The wall teichoic acid and lipoteichoic acid polymers of *Staphylococcus aureus*. *Int. J. Med. Microbiol.* **300**, 148–154 (2010).
10. Lu, Y. et al. Modulation of MRSA virulence gene expression by the wall teichoic acid enzyme TarO. *Nat. Commun.* **14**, 1594 (2023).
11 Labroli, M. A. et al. Discovery of potent wall teichoic acid early stage inhibitors. *Bioorg. Med. Chem. Lett.* **26**(16), 3999–4002 (2016).
12. Campbell, J. et al. Synthetic lethal compound combinations reveal a fundamental connection between wall teichoic acid and peptidoglycan biosyntheses in *Staphylococcus aureus*. *ACS Chem. Biol.* **6**, 106–116 (2010).
13. Weidenmaier, C. et al. Lack of wall teichoic acids in *Staphylococcus aureus* leads to reduced interactions with endothelial cells and to attenuated virulence in a rabbit model of endocarditis. *J. Infect. Dis.* **191**(10), 1771–1777 (2005).
14 Horsburgh, M. et al. Peptidoglycan crosslinking relaxation plays an important role in *Staphylococcus aureus* WalKR-dependent cell viability. *PLoS ONE* **6**, e17054 (2011).
15. Park, J.-M. et al. Rapid screening and comparison of chimeric lysins for antibacterial activity against *Staphylococcus aureus* strains. *Antibiotics* **12**, 667 (2023).
16. Pitkänen, I., Tossavainen, H. & Permi, P. ^{1}H, ^{13}C, and ^{15}N NMR chemical shift assignment of LytM N-terminal domain (residues 26–184). *Biomol. NMR Assign.* **17**, 257–263 (2023).

17. Diarra, M. S. et al. In vitro and in vivo antibacterial activities of cranberry press cake extracts alone or in combination with β-lactams against *Staphylococcus aureus*. *BMC Complement. Altern. Med.* **13**, 90 (2013).
18 Mu, C. et al. The expression of LytM is down-regulated by RNAIII in *Staphylococcus aureus*. *J. Basic Microbiol.* **52**(6), 636–641 (2012).
19. Lee, S. H. et al. TarO-specific inhibitors of wall teichoic acid biosynthesis restore β-lactam efficacy against methicillin-resistant staphylococci. *Sci. Transl. Med.* **8**(329), 329ra32 (2016).
20. Ji, L. Y. et al. Identification of bioactive compounds and potential mechanisms of scutellariae radix-coptidis rhizoma in the treatment of atherosclerosis by integrating network pharmacology and experimental validation. *Biomed. Pharmacother.* **165**, 115210 (2023).
21. Guo, Y., Pfahler, N. M., Völpel, S. L. & Stehle, T. Cell wall glycosylation in *Staphylococcus aureus*: Targeting the tar glycosyltransferases. *Curr. Opin. Struct. Biol.* **68**, 166–174 (2021).
22. Brown, S. et al. Methicillin resistance in *Staphylococcus aureus* requires glycosylated wall teichoic acids. *Proc. Natl. Acad. Sci.* **109**, 18909–18914 (2012).
23. Dubrac, S., Boneca, I. G., Poupel, O. & Msadek, T. New insights into the WalK/WalR (YycG/YycF) essential signal transduction pathway reveal a major role in controlling cell wall metabolism and biofilm formation in *Staphylococcus aureus*. *J. Bacteriol.* **189**, 8257–8269 (2007).
24. Orihuela, C. J. et al. SpdC, a novel virulence factor, controls histidine kinase activity in *Staphylococcus aureus*. *PLOS Pathog.* **14**, e1006917 (2018).
25. Chen, L. et al. Cryo-electron microscopy structure and transport mechanism of a wall teichoic acid ABC transporter. *mBio* **11**(2), e02749-e2819 (2020).
26. Farha, M. A. et al. Inhibition of WTA synthesis blocks the cooperative action of PBPs and sensitizes MRSA to β-lactams. *ACS Chem. Biol.* **8**, 226–233 (2012).
27. CLSI. *Performance Standards for Antimicrobial Susceptibility Testing* M100–M128 (Clinical and Laboratory Standards Institute (CLSI), 2022).
28. Kumarihamy, M. et al. Synthesis and inhibitory activity of machaeridiol-based novel anti-MRSA and anti-VRE compounds and their profiling for cancer-related signaling pathways. *Molecules* **27**(19), 6604 (2022).
29. Ye, J. et al. Novel copper-containing ferrite nanoparticles exert lethality to MRSA by disrupting MRSA cell membrane permeability, depleting intracellular iron ions, and upregulating ROS levels. *Front. Microbiol.* **14**, 1023036 (2023).
30. Prencipe, F. et al. Allantodapsone is a pan-inhibitor of *Staphylococcus aureus* adhesion to fibrinogen, Loricrin, and cytokeratin 10. *Microbiol. Spectr.* **10**(3), e01175-21 (2022).
31. Meredith, T. C., Swoboda, J. G. & Walker, S. Late-stage polyribitol phosphate wall teichoic acid biosynthesis in *Staphylococcus aureus*. *J. Bacteriol.* **190**, 3046–3056 (2008).
32. Liu, M. et al. The direct anti-MRSA effect of emodin via damaging cell membrane. *Appl. Microbiol. Biotechnol.* **99**(18), 7699–7709 (2015).

Acknowledgements
We report no potential conflict of interest.

Author contributions
GXM and ZFF designed the study and wrote the manuscript; JMM and LH formal analysis; LM and DY Investigation; WW and XZB Visualization; XMY and JMM methodology; GXM and ZFF writing-original draft; XMY and WL writing-review and editing; WL funding acquisition. All authors read and approved the final work.

Funding
This work was supported by grants from the Key Discipline of Xuhui District, Shanghai (SHXHZDXK-202322) and the Comprehensive Hospital Traditional Chinese and Western Medicine Integration Special Project of Shanghai (ZHYY-ZXYJHZX-202104) and Jiangsu University Medical Education Collaborative Innovation Fund (JDYY2023121).

Declarations

Competing interests
The authors declare no competing interests.

Additional information
Supplementary Information The online version contains supplementary material available at https://doi.org/10.1038/s41598-025-91724-3.

Correspondence and requests for materials should be addressed to M.X. or L.W.